Rev. Roum. Sci. Techn.– Électrotechn. et Énerg.
Vol. **62**, *2*, pp. 142–147, Bucarest, 2017

EXPERIMENTAL ANALYSIS OF DYNAMIC ECCENTRICITY IN THE INDUCTION MACHINE USING MOTOR CURRENT SIGNATURE ANALISYS AND DISCRETE WAVELET TRANSFORM

AHCENE BOUZIDA[1], RADIA ABDELLI[2], OMAR TOUHAMI[1]

Key words: Induction machine, Eccentricity, Multi-level decomposition, Fault diagnostic, Discrete wavelet transform.

The diagnosis of the dynamic eccentricity faults based on the old analysis techniques, such as the motor current signature analysis (MSCA), suffers from some difficulties and the exactness of those techniques is related to the load, healthy conditions and the ability to maintain a constant speed during the data acquisition process. To overcome this problem, the analysis of the stator current waveform using the discrete wavelet transform has been investigated and a method for the diagnosis of dynamic eccentricity for the induction machine has been presented. It is based on the analysis of the stator current, using the MCSA and the discrete wavelet transform (DWT), in order to extract the different related frequencies and the different energies stored in each level obtained by DWT. The performance offered by using the DWT is the ability to provide an ideal differentiation between the healthy and the eccentric machine.

1. **INTRODUCTION**

The three-phase squirrel cage induction motors are involved in a huge amount of industrial applications where their reliability plays a principal role. A sudden failure of a system in these examples may lead to cost expensive downtime, damage to surrounding equipment or even danger to humans. Therefore, the main goal of the research during these last years is to reduce the maintenance costs. For this, a great importance is done in the field of fault prognosis on induction machines and it's substantially increased as well as the budgets dedicated to that field. Among all the possible faults in induction machines, dynamic eccentricity constitutes an important percentage, as Thomson [1] or Durocher [2] showed. A rotor eccentricity is one of the main mechanical faulty conditions of induction machines. It causes excessive stressing of the machine, increasing bearing wear and amplifying vibrations. It may even cause rotor-stator rub in extreme cases, with consequential damage to the stator winding. Thus, the monitoring of dynamic rotor eccentricities is highly recommended to prevent serious operational failures.

The most widely used approach in the industrial environment for fault diagnosis of this problem is based on analyzing the stator current and its derivatives. This is a quantity feasible to be measured in a simple way. It avoids the necessity of complex data acquisition systems [1].

Certain range of mechanical faults as dynamic eccentricity can be detected by the analyzing of the frequency spectrum of the steady-state current or vibration signal. Nevertheless, the utilization of the current spectrum has some drawbacks. For instance, in the case of dynamic eccentricity, there are some cases in which the detection of this fault using the fast Fourier transform (FFT) is not feasible because of the presence of other phenomena. This happens for instance, when the machine fully loaded or when other phenomena such as voltage oscillations or load torque fluctuations introduce frequencies similar to those associated with the dynamic eccentricity. These conditions make difficult the prognosis and can even lead to wrong results during the diagnosis process if only one approach is used [3].

Many recent works have applied the discrete wavelet transform (DWT) to the stator current in order to detect the presence of dynamic eccentricity in induction machines [4–7]. The DWT is an ideal tool to study signals when the frequency spectrum varies in time, allowing a time-frequency decomposition of the signal to be studied. The objective of those works was to extract the energy of the certain frequency bands provided by the DWT. They act as frequency filters, extracting the evolution of the frequencies included within their associated frequency band. The application of this approach avoids some of the problems of the FFT analysis.

The aim of the present paper is to apply an old technique based on FFT for the detection of dynamic eccentricity in induction machines and a new approach based on DWT, since the frequency components introduced by dynamic eccentricity are dependent on the load condition. Their detection and decision can constitute an effective indicator for the diagnosis of the fault. For this work, the wavelet bands resulting from the decomposition in multi-levels by the DWT are used, due to their orthogonality. The method allows the detection of the presence of the fault information in two different ways; a qualitative one, based on the analyzing of the characteristic pattern that arises in the high-level wavelet signals, and a quantitative approach, based on the analysis of the energy of the signals that are amplified by the fault. This method constitutes an important advantage compared to the traditional tools, in which only the increase in the amplitudes of some particular components is analyzed, being sometimes difficult to explain the reason for a certain increment, that might have been produced by other phenomena, or to distinguish between a healthy and a faulty machine.

2. **DESCRIPTION OF DYNAMIC ECCENTRICITY**

The rotor eccentricity in an induction machine is reflected through a non-uniform air-gap between stator and rotor. The dynamic eccentricity (DE) is present when the rotation axis of the rotor does not coincide with its geometric axis. This fact causes that the position of minimum air-gap changes in time and space. This eccentricity can be due to

[1] M'hamed Bougara University of Boumerdes, Algeria; E-mail: ah_bouzida@univ-boumerdes.dz
[2] University of Bejaia, Abderrahmane Mira, Algeria; E-mail: abdelli_radia@yahoo.fr

reasons such as rotor axis deformation, bearing wear, misalignment or mechanical resonance at critical speed.

Usually the dynamic eccentricity exists for the healthy conditions, being very difficult to find a pure dynamic or load related problems.

In this paper, a dynamic eccentricity will be considered, although a certain degree under various load levels (Fig. 1).

There have been many of papers dealing with the frequency components introduced by the dynamic eccentricity in the current spectrum. The main approaches for the detection of such a fault are detailed. The sideband frequencies associated with an eccentricity are around the slot frequencies and they are given by [9],

$$f_{slot+ecc} = f_1\left[(kR \pm n_d)(\frac{1-s}{p}) \pm n_w\right], \qquad (1)$$

where f_1 is the supply frequency, k = 1, 2, 3..., R is the number of rotor slots, n_d for static eccentricity and 1 for dynamic eccentricity, s – the slip, p – the number of pole pairs, and n_w the order of MMF of stator slot harmonic. The second approach monitors the behaviour of the sideband components around the supply frequency. Their frequencies are given by:

$$f_{ecc} = f_1\left[(1 \pm m)(\frac{1-s}{p})\right], \quad m = 1, 2, 3 \ldots \qquad (2)$$

The first approach makes a possibility of differentiation between the spectral components caused by the eccentricity and those caused by the broken bar, but it needs more detailed information about the machine characteristics [4].

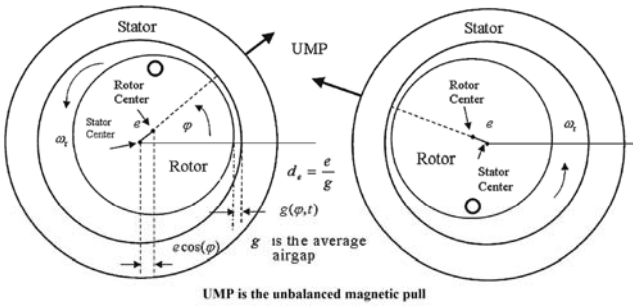

Fig. 1 – Dynamic eccentricity.

3. DISCRETE WAVELET TRANSFORMS (DWT) DESCRIPTION

The wavelet transformation WT is processes of determining how well a series of wavelet functions represent the signal being analyzed. The effectiveness of fitting of the function to the signal is described by the wavelet coefficients. The result is a bank of coefficients associated with two independent variables, dilation and translation. Translation typically represents time, while scale is a way of viewing the frequency content. Larger scale corresponds to lower frequency meaning there by better resolution. The most efficient and compact form of the wavelet analysis is accomplished by decomposing a signal into a subset of translated and dilated parent wavelets, where these various scales and shifts in the parent wavelet are related based on powers of two. Full representation of a signal can be achieved using a vector coefficients which have the same length as the original signal.

A wavelet is a function belonging to $L^2(R)$ with a zero average. It is normalized and centered on the neighborhood of $t = 0$. A time-frequency atom family is obtained by scaling a band pass filter ψ by s and translating it by u.

$L^2(R)$ represents the space vector of measurable square-integrable functions on the real line R with $\|\psi\| = 1$.

$$\int_{-\infty}^{+\infty} \psi(t)\mathrm{d}t = 0, \qquad (3)$$

$$\psi_{u,s}(t) = \frac{1}{\sqrt{s}}\psi(\frac{t-u}{s}). \qquad (4)$$

The wavelet transform of a function f at the scale s and position u is computed by correlating f with a wavelet atom:

$$Wf(u,s) = \int_{-\infty}^{+\infty} f(t)\frac{1}{\sqrt{s}}\psi(\frac{t-u}{s})\mathrm{d}t, \qquad (5)$$

when $Wf(u,s)$ is known only for $s<s_0$, we need to recover f, a complement of information corresponding to $Wf(u,s)$ for $s>s_0$. This is obtained by introducing a scaling function φ that is a wavelets aggregate at scales larger than 1. In the sequel, we design by $\hat{\psi}(\omega)$ and $\hat{\varphi}(\omega)$ the Fourier transforms of $\psi(\omega)$ and $\varphi(\omega)$, respectively.

The discrete wavelets transform results from the continuous version. Unlike this latter, the DWT uses a discrete scale factor and a translation. We call discrete wavelet transform dyadic any base of wavelet working with a scale factor $u = 2^j$.

The discrete wavelets transform can be obtained from the continuous version. It uses a discrete scale factor and a translation and working with a scale factor into any bases.

The discrete version of wavelet transform, DWT, consists of sampling neither the signal nor the transform but sampling the scaling and shifted parameters [12, 13]. This results in high frequency resolution at low frequencies and high time resolution at high frequencies, removing the redundant information. Taking positive frequency into account, $\hat{\psi}(\omega)$ has information in $[0, \pi]$ and $\hat{\varphi}(\omega)$ in $[0, 2\pi]$. Therefore, they both have complete signal information without any redundancy. Functions $h(n)$ and $g(n)$ can be obtained by the inner product of $\psi(\omega)$ and $\varphi(\omega)$. The decomposition of the signal in $[0, \pi]$ gives [4, 10, 11]

$$\begin{aligned} h(n) &= \left\langle 2^{-l}\varphi(2^{-l}t)\varphi(t-n)\right\rangle \\ g(n) &= \left\langle 2^{-j}\psi(2^{-j}t)\varphi(t-n)\right\rangle, j = 0, 1, \ldots, \end{aligned} \qquad (6)$$

Wavelet decomposition does not involve the signal in $[\pi, 2\pi]$. In order to decompose the signal in the whole frequency band, wavelet packets can be used. After decomposing l times, we get 2^l frequency bands each with the same bandwidth that is:

$$\left[\frac{(i-l)f_n}{2}, \frac{if_n}{n}\right], \quad i = 1, 2, \ldots, 2^l, \qquad (7)$$

where f_n is the Nyquist frequency, in the i^{th}-frequency band. Wavelet decompose the signal into one low-pass filter $h(n)$

and 2^{l-1} band-pass filters $g(n)$, and provide diagnosis information in 2 frequency bands. A_j is the low frequency approximation and D_j is the high frequency detail signal, both at the resolution j:

$$A_j(n) = \sum_k h(k-2n)A_{j-1}(k)$$
$$D_j(n) = \sum_k g(k-2n)A_{j-1}(k), \quad (8)$$

where $A_0(k)$ is the original signal. After decomposing the signal, we obtain one approximation signal Aj and Dj detail signals (see Fig.2).

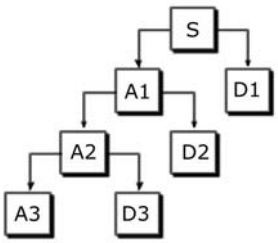

Fig. 2 – Tree decomposition of the signal S using DWT.

4. EXPERIMENTAL SETUP

For an induction machine, the significant information in the stator current signal for mechanical faults is concentrated in the low and high bands of frequency. Applying the Shannon's theorem, yields high sampling frequency.

The minimum resolution needed to get a good result is defined by (9), where the number of samples, Ns, needed for a given resolution R [14, 15], $N_s = \frac{f_s}{R}$.

In our case, we have chosen a sampling frequency f_s = 26.5 kHz and Ns = 507 904 samples to obtain a good frequency resolution R = 0.0522. The analyzing frequencies vary from 0 to 13.25 kHz with a high resolution.

Figure 3 shows the experimental setup where the induction machines are used to test the performance of the proposed methodology identifying the fault treated in this work. This system can be used to sample currents I_a, I_b, and I_c, three line voltages V_a, V_b and V_c, and a speed signal. The stator windings are star connected. The main parts of the experimental setup are as follows:

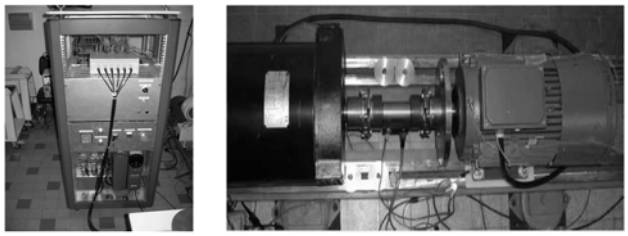

Fig. 3 – Experimental setup.

- three-phase 5.5 kW induction machine,
- dc-ac converter 400 V,
- dc generator coupled to the induction machine to provide load,
- PC equipped with a data acquisition card.

Table 1

The tested machine characteristics

Rated power	5.5 kW
Rated frequency	50 Hz
Connection	Y
Rated current	10.5 A
Voltage	400 V
Rated speed	1445 rpm
Number of stator slots	48
Number of rotor slots	28
Rated torque	35 Nm
Efficiency	87%

The machine is tested under 3 steps of load:
- Case A: 30 % rated load.
- Case B: 50 % rated load.
- Case C: 75 % rated load.

Figure 4 shows the acquired line current I_a using the acquisition card with the sampling frequency of 25.6 kHz.

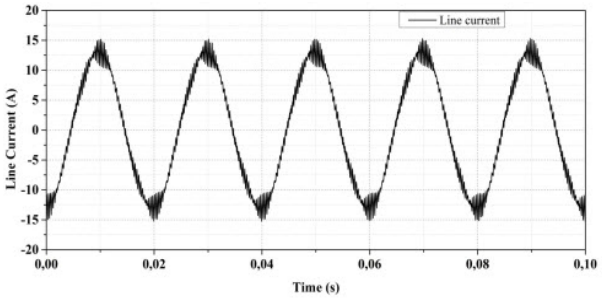

Fig. 4 – Measured line current I_a.

The extraction of the fundamental component leads to a signal full of inside information. Indeed the elimination of the dominant component in the stator current contributes to amplify the components due to dynamic eccentricity. For this reason we make the stator current go through a band-pass filter to eliminate the 50 Hz frequency. This method can produce attenuation in some frequency components.

The side-bands of the rotor rotational frequency normalized to the 50 Hz components under 50 % DE conditions at 30 %, 50 % and 75 % of rated load are shown in Figs. 6, 7 and 8. The expectation was that the side-bands would increase in the case of the DE. However, it can be seen that the measurements are inconsistent, and the amplitude of the components ($f_s \pm kf_r$) depends on the load level. The inconsistency can be attributed to other factors such as misalignment, load unbalance, or oscillating load that produce components larger than that due to dynamic eccentricity at the same frequency [16–18].

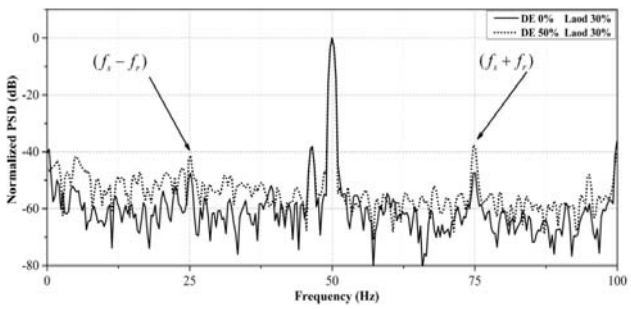

Fig. 5 – Normalized power spectrum density of stator current for case A.

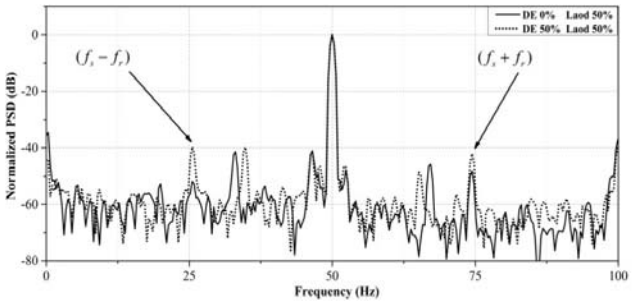

Fig. 6 – Normalized power spectrum density of stator current for case B.

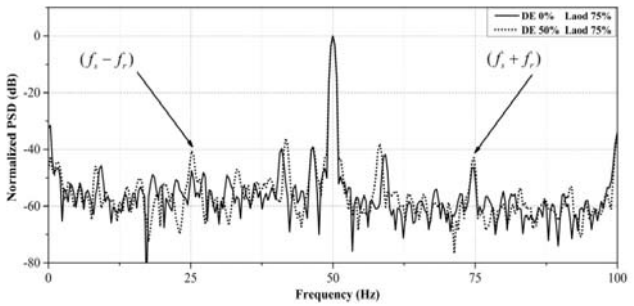

Fig. 7 – Normalized power spectrum density of stator current for case C.

The normalized power spectrum density (PSD) of the stator current for the tested machines with 50 % DE at 30 %, 50 % and 75 % rated load are shown in Figs. 5, 6, and 7. For the DE cases under 30 %, 50 % and 75 % of rated load, the increasing in the amplitude of the components $(f_s - f_r)$ and $(f_s + f_r)$ can be clearly observed. The Table 2 summarizes the various amplitudes of the spectral components $(f_s \pm f_r)$ for the different cases. The increase of the amplitudes can be caused by a combined effect of the natural eccentricities related to the manufacturing phase, oscillations of the load and shaft misalignment. Therefore, it is very difficult for the maintenance engineer to conclude with confidence based on this approach that airgap eccentricity is present in the machine.

Table 2

Amplitudes of the $(f_s + f_r)$ components

Indicator		Load = 30 %		Load = 50 %		Load = 75 %	
	DE %	0 %	50 %	0 %	50 %	0 %	50 %
$(f_s - f_r)$	Hz	25.15	25.15	25.49	25.49	25.15	25.15
	dB	- 47.48	- 41.22	- 51.92	- 39.69	- 46,56	- 40.71
$(f_s + f_r)$	Hz	74.77	74.77	74.34	74.32	74.77	74.77
	dB	- 47.29	- 37.77	- 48.14	- 42.10	- 46.23	- 42.81

The experimental test shows also a various difficulties to detect the dynamic eccentricity, because the components $(f_s - f_r)$ are observed for all cases including those corresponding to the healthy machine. Hence, in the same process of diagnosis the knowledge of the healthy conditions is necessary. For this reason, the criterion of distinction between a healthy and defective machine will be based on the amplitude of these components.

5. SPECIFICATION OF THE NUMBER OF DECOMPOSITION LEVELS

We have experimented a method for the selection of wavelet decomposition level namely the approach presented in [4], the approach is based on a suitable number of decomposition levels n_{Ls} witch depends on the sampling frequency f_s of the stator current.

The minimum number of decomposition levels that is necessary for obtaining an approximation signal A_{nf} so that the upper limit of its associated frequency band is under the fundamental frequency [16], is described by the following condition:

$$2^{-(n_{ls}+1)} f_s < f \,. \tag{9}$$

From this condition, the decomposition level of the approximation signal which includes the left side-band harmonic is the integer n_{ls} given by:

$$n_{ls} = \text{int}\frac{\log(f_s / f)}{\log(2)} \,. \tag{10}$$

For this case the wavelet decomposition tree is shown in Table 3.

Table 3

Frequency bands obtained by decomposition in multilevel

Level	Approximations [Hz]			Details [Hz]
J = 1	A1	0 - 13250	D1	13250 - 26500
J = 2	A2	0 - 6625	D2	6625- 13250
J = 3	A3	0 – 3312.5	D3	3312.5- 6625
J = 4	A4	0 – 1656.2	D4	1656.25- 3312.5
J = 5	A5	0 – 828.12	D5	828.12- 1656.25
J = 6	A6	0 - 414	D6	414- 828.125
J = 7	A7	0 - 207	D7	207- 414
J = 8	A8	0 -103.5	D8	103.5- 207
J = 9	A9	0 – 51.75	D9	51.75- 103.5
J = 10	A10	0 – 25.87	D10	25.875- 51.75
J = 11	A11	0 – 12.94	D11	12.94- 25.87

Many mother wavelets types can be used to analyze the stator current and have different properties. However, some applications showed that all these types of mother wavelets gave similar results. Due to the well-known properties of the orthogonal Daubechies family, we chose to use a mother wavelet of this family.

The Daubechies wavelets db8 is used to decompose the residual stator current of the machine for the different cases. Figures 8 and 9 represent the detail, and the approximation signals (D11, D10, D9 and D8) obtained by db8 for the healthy and eccentric machines under 30 % of rated load.

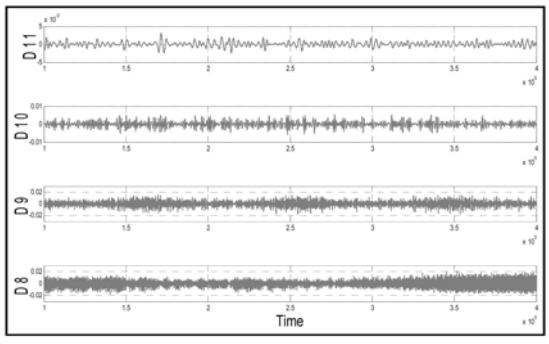

Fig. 8 – Details and approximations for healthy machine case A.

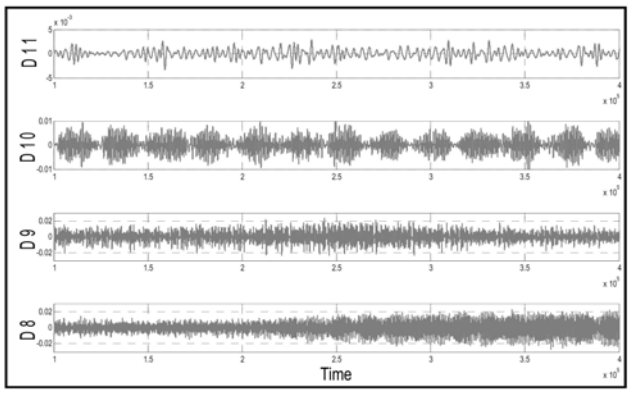

Fig. 9 – Details and approximations for eccentric machine case A.

In Figs. 8 and 9, the evolution in the observed frequency bands of the relative signal to the dynamic eccentricity can be analyzed using coefficients D11, D10, D9 and D8. While analyzing the effect of the dynamic eccentricity in the bands of interesting frequencies, we show that the energy depends on the defect. For the studied machine, the difference between the healthy and the eccentric machines is clearly shown in Fig. 9.

The multilevel decomposition of the filtered stator current was then performed using Daubechies wavelet, the suitable level of decomposition is calculated according to Eq. (11). When the defect of dynamic eccentricity in the induction motor appears, the defect information in stator current is included in each frequency band determined by the decomposition in wavelet tree. By calculating the energy associated with each level or with the each node of decomposition, we can build a very effective diagnosis tool. The energy eigenvalue for each frequency band is defined by [14, 15]:

$$E_j = \sum_{k=1}^{k=n} \left| D_{j,k}(n) \right|^2 , \tag{11}$$

$$T = \left[\frac{E_0}{E}, \frac{E_1}{E}, \frac{E_2}{E}, ..., \frac{E_{2^l-1}}{E} \right], \tag{12}$$

Where j = 1, 2…, $2^l - 1$; D_j is the amplitude in each discrete point of the wavelet coefficient of the signal in the corresponding frequency band, with:

$$E = \sum_{j=0}^{2^m-1} \left| E_j \right|^2 . \tag{13}$$

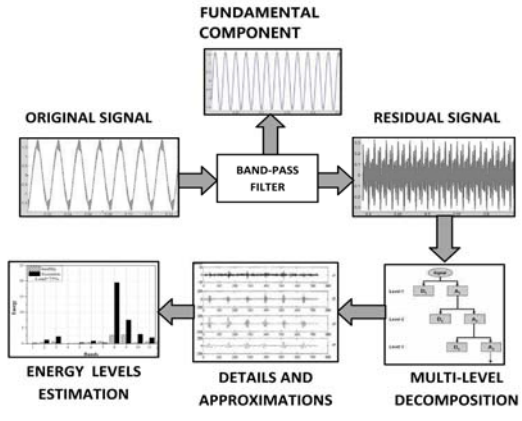

Fig. 10 – Eigenvector analysis.

The eigenvalue T contains information on the signal of the filtered stator current for a motor behavior. Besides, the amplitudes of the deviation of some eigenvalues indicate the presence of the defect, which makes T a good candidate to diagnose dynamic eccentricity.

Figures 11, 12 and 13 represent the variation of the energy eigenvalue.

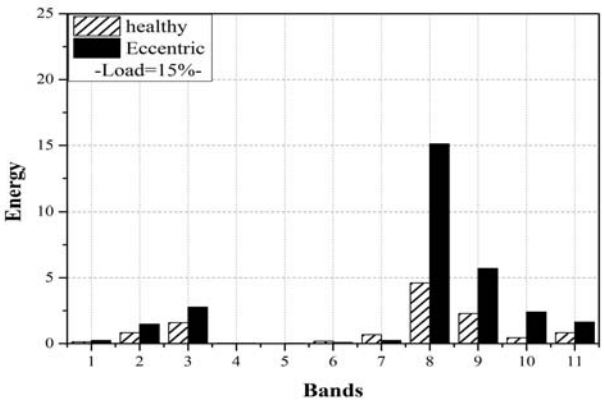

Fig. 11 – Eigenvector analysis results obtained for case A.

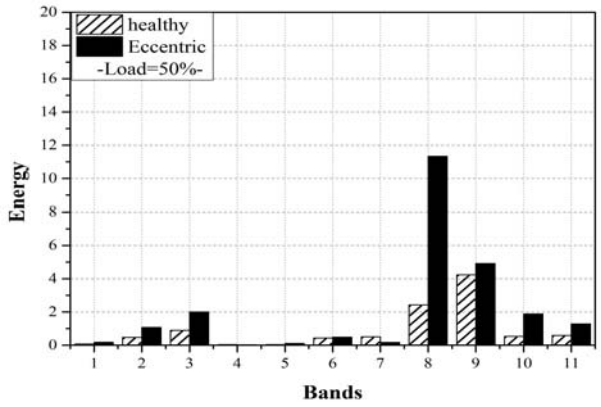

Fig. 12 – Eigenvector analysis results obtained for case B.

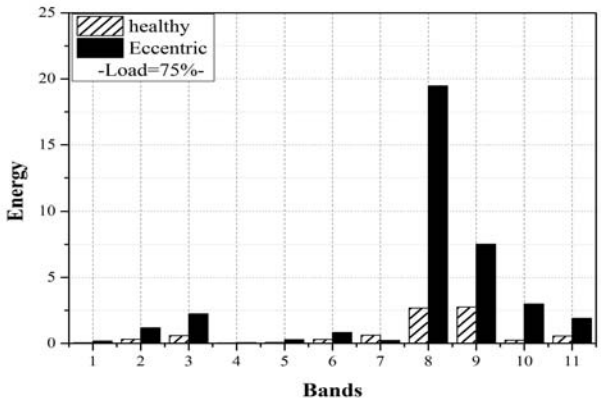

Fig. 13 – Eigenvector analysis results obtained for case C.

The figures clearly show the variation of the energy eigenvalue for the three cases A, B and C. We can observe that the energy stored in bands 2, 3, 8, 9, 10 and 11 shows the difference between the healthy and faulty machine, the energy in levels 8, 9, 10 and 11 represents the band where the significant information in the stator current signal is concentrated the 0 – 400 Hz. However the energy eigenvalue depends on the load step, but the differentiation between the healthy and faulty machine is also possible.

The band of detection of dynamic eccentricity can be

influenced by the mechanical vibrations and the load effect as the frequencies accompanying the mechanical problems are superposed in the band of detection which is located in 0 – 414 Hz. The dynamic eccentricity induces supplementary frequencies near the fundamental component which are described by ($f_s \pm f_r$). These frequencies are influenced by the operating frequency f_s and the slip s, however this method is not dependent on the motor power, but we must choose the appropriate band and the decomposition of the stator current.

6. **CONCLUSION**

MCSA is a good approach for analyzing mechanical faults over constant load. But for the case of non-symmetric load or mixed faults, the use of the wavelet decomposition approach is required.

This paper investigates the detection of dynamic eccentricity using wavelet analysis of the current. The wavelet technique presented here is able to extract useful characteristics from the stator current of an induction motor under a large frequency band.

The results of wavelet transformation give the valuable information to decide the faulty case, particularly in the presence of dynamic eccentricity and the number of acquisition points is very important. This method can clearly exhibit the time-frequency characteristic of fault signals, by increasing the energy in different frequency bands obtained by the decomposition in multi-level. The proposed method provides a promising way for the mixed-faults diagnosis of induction motors.

Received on February 10, 2016

REFERENCES

1. W.T. Thomson, M. Fenger, *Current signature analysis to detect induction motor faults*, IEEE Industry Applications Magazine, pp. 26–34, 2001.
2. D.B. Durocher, G.R. Feldmeier, *Predictive versus preventive maintenance*, IEEE Industry Applications Magazine, **10**, 5, pp. 12–21, 2004.
3. J. Antonino-Daviua, P. Joverb, M. Rieraa, A. Arkkiob, J. Roger-Folcha, *DWT analysis of numerical and experimental data for the diagnosis of dynamic eccentricities in induction motors*, Mechanical Systems and Signal Processing, **21**, *6*, pp. 2575–2589, 2007.
4. Khadim Main Siddiqui, V.K Giri, *Broken Rotor Bar Fault Detection in Induction Motors Using Wavelet Transform*, International Conference on Computing, Electronics and Electrical Technologies (ICCEET), 2012.
5. J. Ridha Kechida, Arezki Menacer, *Application of the Fourier and the Wavelet Transform for the Fault Detection in Induction Motors at the Startup Electromagnetic Torque*, 2nd International Conference on Electric Power and Energy Conversion Systems (EPECS), 2011.
6. Arezki Menacer, Ridha Kechida, Gérard Champenois, Slim Tnani., *DWT wavelet transform for the rotor bars faults detection in induction motor*, 2nd International Conference on Electric Power and Energy Conversion Systems (EPECS), 20011.
7. J. Seshadrinath, B. Singh, B.K. Panigrahi, *Single-Turn Fault Detection in Induction Machine Using Complex-Wavelet-Based Method*, IEEE Transactions on Industry Applications, **48**, *6*, pp. 1846–1854, 2012.
8. S. Nandi, H.A. Toliyat, *Condition monitoring and fault diagnosis of electrical motors – A review*, IEEE Transactions on Energy Conversion, **20**, *4*, pp. 719–729, 2005.
9. M.H. Benbouzid, *A review of induction motors signature analysis as a medium for faults detection*, IEEE Transactions on Industrial Electronics, **47**, *5*, pp. 0278–0046, 2000.
10. M.E.H. Benbouzid , G.B. Kliman, *What stator current processing based technique to use for induction motor rotor faults diagnosis*, IEEE Trans. Power Del, **19**, *3*, pp. 957–964, 2004.
11. T. Tarasiuk, *Hybrid wavelet-Fourier spectrum analysis*, IEEE Transactions on Energy Conversion, **18**, *2*, pp. 238–244, 2003.
12. Supangat, N. Ertugrul, W.L. Soong, D.A. Gray, C. Hansen, J. Grieger, *Detection of broken rotor bars in induction motor using starting-current analysis and effects of loading*, Proc. Inst. Elect. Eng. Elect. Power Appl, **153**, *6*, pp. 848–855, 2006.
13. P. Rodriguez, *Current-force- and vibration based techniques for induction motor condition monitoring*, Ph.D. Dissertation, Helsinki Univ. Technol., Espoo, Finland, 2007.
14. Z. Cvetkovic, M. Vetterli, *Discrete-time wavelet extrema representation: Design and consistent reconstruction*, IEEE Trans. Signal Process, **43**, *3*, pp. 681–693, 1995.
15. T.W.S. Chow, S. Hai, *Induction machine fault diagnostic analysis with wavelet technique*, IEEE Trans. Ind. Electron, **51**, *3*, pp. 558–565, 2004.
16. L. Wu, X. Huang, T.G. Habetler, R.G. Harley, *Eliminating load oscillation effects for rotor eccentricity detection in closed-loop drive connected induction motors*, IEEE Trans. on Pwr. Electr, **22**, *4*, pp. 1543–1551, 2007.
17. R.R. Obaid, T.G. Habetler, *Current-based algorithm for mechanical fault detection in induction motors with arbitrary load conditions*, Proc. of IEEE IAS Annual Meeting, **38**, *2*, pp. 1347–1351, 2003.
18. R.R. Schoen, T.G. Habetler, *Effect of time-varying loads on rotor fault detection in induction machines*, IEEE Trans. on Ind. Appl, **31**, *4*, pp. 900–906, 1995.
19. A.H. Boudinar, N. Benouzza, A. Bendiabdellah, *Diagnostic des Défauts de Roulements d'un Moteur Asynchrone*, Rev. Roum. Sci. Techn. – Électrotechn. et Énerg., **60**, *1*, pp. 39–48, 2015.